Direct Power Control of DFIG Wind Turbine Systems Based on an Intelligent Proportional-Integral Sliding Mode Control

Shanzhi Li[a], Haoping Wang[a*], Yang Tian[a], Abdel Aitouch[b], John Klein[b]

[a] *LaFCAS, School of Automation, Nanjing University of Science and Technology, Nanjing,210094, China*

[b] *CRIStAL UMR CNRS 9189, University of Lille 1, France*

Abstract- This paper presents an intelligent proportional-integral sliding mode control (iPISMC) for direct power control of variable speed-constant frequency wind turbine system. This approach deals with optimal power production (in the maximum power point tracking sense) under several disturbance factors such as turbulent wind. This controller is made of two sub-components: (i) an intelligent proportional-integral module for online disturbance compensation and (ii) a sliding mode module for circumventing disturbance estimation errors. This iPISMC method has been tested on FAST/Simulink platform of a 5MW wind turbine system. The obtained results demonstrate that the proposed iPISMC method outperforms the classical PI and intelligent proportional-integral control (iPI) in terms of both active power and response time.

Keywords: Wind turbine system; Model-free control; Sliding mode control

1. INTRODUCTION

As a consequence of population expansion and increasing environmental issues, the demand for renewable energy generation systems keeps growing. As a green and clean energy, wind turbine systems have been paid considerable attention and their proportion in nationwide energy production will rise in the next decade according to the Global Wind Energy Council report [1, 2]. However, random wind fluctuations and wind turbine nonlinearity are major difficulties for exploiting renewable energy with a high efficiency. The nonlinear characteristics of a wind turbine system can be classified as electrical and mechanical nonlinearities. While the former are related to the generators and its uncertain parameters; the latter are related to the drive train and wind wheels for instance. Considering both electrical and mechanical nonlinearities, designing an efficient wind turbine controller is a challenging problem.

Wind turbine systems are high-order nonlinear systems. The doubly fed induction generator (DFIG) is widely utilized on the multi-MW wind turbines because of its low cost and small size. Their nonlinear characteristics are not only reflected in the DFIG model, but also in the aerodynamic and drive-train models. With large power wind

* Corresponding author: hp.wang@njust.edu.cn

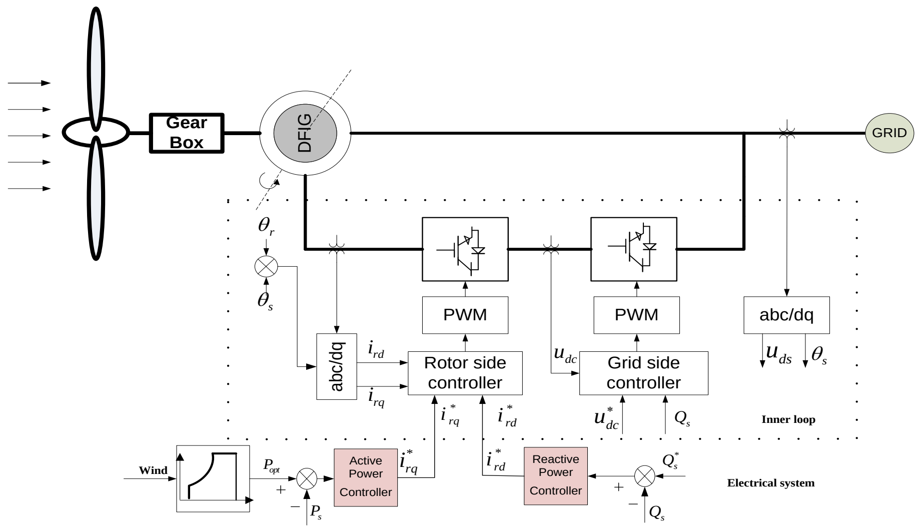

Fig. 1. The DFIG wind turbine system

turbine systems developing and blade diameter increasing, its nonlinear feature will be reinforced, and will influence directly the output performance of wind turbine systems.

Modeling and control of wind turbine systems has been a vivid research topic in the past decade [3]. A controller can optimize the power production of a DFIG in many ways. For speed and torque or power control of DFIGs, there are vector control, direct torque control and direct power control [4].

In low wind speed region (between cut-in speed and rating speed), most of reported methods in the literature aim at tracking the maximum power point (MPP) of DFIGs. In reference [5], a direct power control strategy based on proportional-integral (PI) controller has been developed for DFIGs. Even though this method ensures an input-to-state closed-loop stability, it does not take electrical nonlinearities into account. Considering electrical nonlinearities which are originated in DFIG parameter uncertainties both in resistance and inductance, a sliding mode control approach has been proposed for regulation of the active and reactive power in [6]. In order to circumvent external uncertainty sources such as wind turbulences, a robust fuzzy controller and a fuzzy logic controller for direct power regulation are designed in [7] and [8]. Another type of controller is introduced in [9, 10] for MPP tracking. They use a radial-basis function neural network controller which focuses only on the nonlinear aerodynamic model and neglects the electrical torque equation. The same nonlinear aspects of the aerodynamic model are also taken into account in [11] using the same family of controllers as in [6], i.e. sliding mode controllers. Also in [12], a discrete-time sliding mode approach is introduced for variable speed wind turbine system.

In order to improve the efficiency of MPP tracking, a novel controller relying on an intelligent proportional-integral-derivative (iPID) control is proposed in [13], it has been proved to produce efficient control for a variety of systems such as a quadrotor vehicle [14], DC/DC converters, and motors [15]. This approach uses an observer which is based on algebraic techniques to estimate the unknown dynamics [16]. However, this algebraic based iPID control cannot ensure the trajectory tracking error to tend to zero rapidly. In addition, its estimation performances are significantly degraded by measurement noises [17].

In order to overcome the aforementioned difficulties, this paper presents an extended state observer based intelligent proportional-integral sliding mode control (iPISMC) to perform direct power control of DFIG Wind turbine systems. The extended state observer (ESO) is integrated into an intelligent proportional-integral (iPI) to estimate the unknown uncertain dynamics of the system. An acceptable performance can be ensured when the unknown dynamic is bounded and the parameters of ESO observer are carefully selected [18]. Unfortunately, there always remains a non-null estimation error if the ESO observer is not well selected. Concerning this estimation error, an auxiliary sliding mode controller is added to the ESO based iPI control. The full control strategy that we propose will be referred to as iPISMC. With application of the Lyapunov stability theory, we prove the stability of the proposed iPISMC control. Using simulations generated by the FAST/simulink platform, we show that the proposed controller is robust to random wind inputs and parameter variations. The experiments also demonstrate that iPISMC outperforms PI and iPI controllers in terms of average power production. Note that our goal in this paper is not to prove that iPISMC outperforms any other controller but only to validate that for given proportional and integral gain values, it should be preferred to PI or iPI controllers.

The paper is organized as follows. In section II, wind turbine system modeling and the basic principle of vector control for DFIG will be briefly presented.

In Section III, an intelligent proportional and integral sliding mode controller is designed. Some simulation results are shown in Section IV assessing the quality of iPISMC in terms of power production and response time. At last, section V concludes the paper.

2. Wind turbine system modeling and vector control

The DFIG based wind turbine system which is illustrated in Fig. 1, is mainly composed of the following three components: the aerodynamic subsystem, the DFIG subsystem, and the drive-train subsystem. From Fig. 1, one notes that the general control strategy is based on two loops: the inner loop which regulates the rotor current, and the outer loop which is applied to track the maximum power point. The aerodynamic and gearbox subsystems will be simulated by the FAST platform which is developed by the National Renewable Energy Laboratory (NREL). In this paper, we focus on the maximum power point tracking.

2.1 Aerodynamic subsystem

Usually, the approximate values of aerodynamic power P_a and torque T_a are given by the following equations:

$$\begin{cases} P_a = \dfrac{1}{2}\rho\pi R^2 v^3 C_p(\lambda,\beta) \\ T_a = \dfrac{1}{2}\rho\pi R^3 v^2 C_p(\lambda,\beta)/\lambda \end{cases} \tag{1}$$

where λ is tip speed ratio and we have $\lambda = \omega_m R/v$. R is the blade radius, v is the wind speed, ρ is the air density, β is the pitch angle and C_p is the power coefficient. ω_m is the rotor speed.

In a variable pitch and variable speed system, by changing pitch angle, when wind flows through wind turbine, its output power will be varying with respect to rotor speed and pitch angle. In order to obtain more energy under a given pitch angle value, we can set λ as an optimal value so that the power coefficient can reach a maximum value. Therefore, one typical method for tracking the maximum power is to maintain the tip speed ratio constant by measuring the wind speed and rotor speed [19, 20].

2.2 DFIG subsystem

The induction generator can be written in ***dq*** arbitrary reference frame as follows [21]:

$$\begin{cases} u_{sd} = R_s i_{sd} - \omega_s i_{sd} + \dot{\psi}_{sd} \\ u_{sq} = R_s i_{sq} + \omega_s i_{sq} + \dot{\psi}_{sq} \\ u_{rd} = R_s i_{rd} - \omega_r i_{rd} + \dot{\psi}_{rd} \\ u_{rq} = R_s i_{rq} + \omega_r i_{rq} + \dot{\psi}_{rq} \end{cases}, \tag{2}$$

where $\dot{\psi}_{sd}, \dot{\psi}_{sq}, \dot{\psi}_{rd}, \dot{\psi}_{rq}$ are the derivatives of fluxes $\psi_{sd}, \psi_{sq}, \psi_{rd}, \psi_{rq}$, respectively.

2.3 Drive train subsystem

In the DFIG subsystem, the aerodynamic torque is transferred to generator side by the gearbox. The drive train subsystem can be simplified regardless of friction loss. It can be written as follows [22]:

$$T_a - T_e = J\dot{\omega}_m + B\omega_m, \tag{3}$$

where T_a is the equivalent aerodynamic torque, J is the equivalent moment of inertia and B is damping factor. T_e is the electromagnetic torque.

2.4 Vector Control Strategy of the DFIG based wind turbine system

In order to regulate the power of the DFIG based wind turbine system, a common method is to utilize a vector control by flux orientation, such as stator flux orientation (SFO) [23], stator voltage orientation (SVO). By ***dq*** coordinate transformation, lots of methods can be developed and their controllers are powerful in different aspects. In fact, the differences between these methods are on the control strategy and measured variables [24]. Here, the chosen method for DFIG power regulation is SFO. In steady conditions, voltage and frequency are approximately constant and one has the following relationships

$$\begin{cases} \psi_{sd} = \psi, \psi_{sq} = 0 \\ u_{sq} = \omega_1 \psi, u_{sd} = 0 \end{cases}. \tag{4}$$

By making substitutions in equation (2) using (4), the equivalent rotor dynamic models can be derived as

$$\begin{cases} \dot{i}_{rd} = -(R_r i_{rd} - \omega_r i_{rq}) / \delta L_r + u_{rd} / \delta L_r \\ \dot{i}_{rq} = -(R_r i_{rq} + \omega_r i_{rd}) / \delta L_r + u_{rq} / \delta L_r - \omega_r (L_m / L_s) \psi \end{cases}, \tag{5}$$

where $\delta = 1 - L_m^2 / (L_r L_s)$ is a leak coefficient and ω_r is the rotor electrical speed in the synchronous reference frame. Equation (5) indicates that the current of ***d*** or ***q*** axis is not strictly independent of ***d*** or ***q*** voltage in rotor side.

To perform the decoupled control and achieve high-performance, two different offset voltages will be added to ***dq*** voltages as illustrated in Fig. 2.

The offset voltages can be calculated as

$$\begin{cases} \Delta u_{rd} = -\omega_r \delta L_r i_{rq} \\ \Delta u_{rq} = \omega_r \delta L_r i_{rd} + \omega_r (L_m / L_s) \psi \end{cases}. \tag{6}$$

With the offset voltages, the model of DFIG will be simplified and decoupled. The parameter of inner-loop proportional-Integral controller can be designed according to pole placement. This scheme is used assuming that the stator voltage is fixed and that the compensated voltage can annihilate completely the offset. However, in practice, the performance of a PI controller designed by that method depends on its invariance with respect to system parameters whose values must be known beforehand. Besides, the measurement noise, flux saturation and other nonlinear factors will also increase power error.

The structure of active and reactive power control is shown in Fig. 3. It can be treated as inner loop and outer loop control. The main objective for the outer loop is to regulate active and reactive powers. The output of the outer loop will serve as a reference for the inner loop.

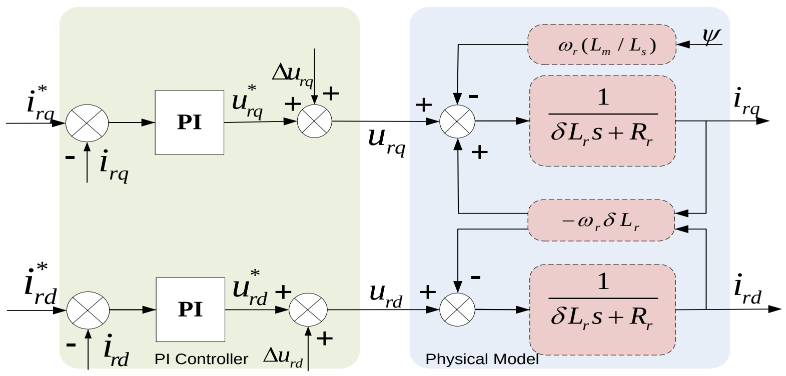

Fig. 2. DFIG model in ***dq*** reference frame

3. Intelligent proportional-integral Sliding Mode Control

In this part, the basic principle of iPI and iPISMC is introduced. The stability of iPISMC in closed-loop system is proved.

3.1 Intelligent proportional-integral Control

For a general single input single output (SISO) nonlinear system, an ultra-local model which is defined as follows can be used to define its corresponding dynamics

$$y^{(n)} = F + \alpha \cdot u\,, \tag{7}$$

where $n \geqslant 1$ is the derivative order of the output y, and u is the input, α is the input gain,. F is the lumped unknown dynamics (LUD) disturbance. If n = 1, a first-order system can be selected to describe the dynamics of the controlled system.

If F and α are well-known items, an iPI control can be proposed as

$$u = \frac{1}{\alpha}(-F + \dot{y}{*} + k_p e + k_i \int edt)\,, \tag{8}$$

where $e = y^* - y$ is the output error and y^* is the desired reference. Substituting equation (8) into (7), the error equation can be deduced as follows

$$\dot{e} + k_p e + k_i \int edt = 0. \tag{9}$$

The steady error dynamics of this closed loop is determined by the parameters k_p and k_i, whose values can be selected according to the Hurwitz criterion.

Let us now fit this model to our electro-mechanical system. Combining the equations (2,4) and (5), the active and reactive powers are calculated as follows

$$\begin{cases} P_s = \frac{3}{2}(u_{sd}i_{sd} + u_{sq}i_{sq}) = \frac{3}{2}\frac{L_m}{L_s}u_{sq}i_{rq} \\ Q_s = \frac{3}{2}(u_{sq}i_{sd} - u_{sd}i_{sq}) = \frac{3}{2}\frac{\psi - i_{rd}L_m}{L_s}u_{sq} \end{cases}, \tag{10}$$

The active and reactive powers are decoupled and they are only related to ***d*** axis or ***q*** axis rotor current. The same iPI controller is retrieved for the active and reactive powers.

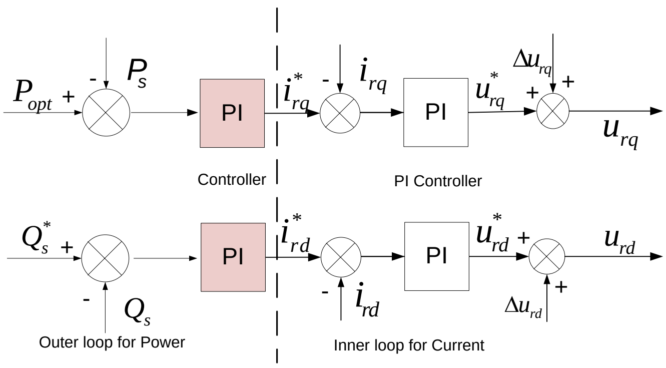

Fig. 3. Two loop vector control for DFIG (PI for Current, PI for Power)

Here, we only explain for the active power case. According to equation (10), the dynamic active power equation can be approximately written as

$$\dot{P}_s = F + \alpha \cdot i_{rq}, \tag{11}$$

where F is a disturbance related to turbulent wind and other factors such as ***d*** axis coupled current, and $\alpha=1.5L_m u_{sq}/L_s$.
The power error is defined as

$$e = P_{opt} - P_s, \tag{12}$$

where P_{opt} is the optimal power obtained on the power chart.
In this paper, the estimated disturbance $\hat{F}$ will be obtained using an extended state observer (ESO) method [25]. According to the ESO method, a second observer is introduced

$$\begin{cases} e_1 = z_1 - P_s \\ \dot{z}_1 = z_2 - \beta_1 e_1 + \alpha u \\ \dot{z}_2 = -\beta_2 \left|e_1\right|^{1/2} sign(e_1) \\ \hat{F} = z_2 \end{cases}, \tag{13}$$

where β_1, β_2 are constant. e_1 is the estimation error of ESO. z_1 and z_2 are the intermediate states. In the ESO framework, z_2 represents the estimation produced by the observer, we thus have $z_2 = \hat{F}$. Therefore, for the first order system (18), the following relatively simple intelligent PI (iPI) control can be proposed to achieve optimal power tracking

$$i_{rq} = \frac{1}{\alpha}(-\hat{F} + \dot{P}_{opt} + k_p \cdot e + k_i \cdot \int e d\tau). \tag{14}$$

From the ESO equations, the estimated error exists and is defined as $\tilde{F} = F - \hat{F}$.

From reference [18], one has generally $\left\|\tilde{F}\right\| \leq f_m$ with f_m an upper bound value.

Substituting equation (14) into (11), the error equation is deduced as

$$\dot{e} + k_p \cdot e + k_i \cdot \int e dt + \tilde{F} = 0. \tag{15}$$

Applying the Laplace transform to equation (15), we obtain:

$$(s + k_p + k_i / s)E(s) + \tilde{F}(s) - \tilde{F}(0^+) = 0. \tag{16}$$

According to final value theorem, the steady error can be calculated as

$$e(t_\infty) = \lim_{t\to\infty} e(t) = \lim_{s\to 0} \frac{s^2}{s^2 + k_p \cdot s + k_i}(\tilde{F}(0^+) - \tilde{F}(s)). \tag{17}$$

Since $\left\|\tilde{F}\right\|$ is bounded and k_p and k_i are selected as Hurwitz polynomial parameters, the steady error $e(t_\infty)$ is ensured to tend to zero. According to the steady error equation (17), the performance of iPI controller depends on the gains k_p and k_i and on the estimated value of F. If the result of the observer is not accurate, this method will be ineffective. In addition, the measurement noise of power will also weaken the performance because estimation error will increase, especially in presence of high-frequency noise.

3.2 Intelligent Proportional-integral Sliding Mode Control

In this part, we add an extra input to compensate the estimation error and measurement noise. The structure of this iPISMC control is shown in Fig 4.

The extra input is denoted by u_e. The final intelligent proportional and integral sliding mode controller (iPISMC) can be defined as

$$i_{rq} = \frac{1}{\alpha}(-\hat{F} + \dot{P}_{opt}^{*} + k_p \cdot \mathrm{e} + k_i \cdot \int ed\tau) + u_{\mathrm{e}} . \tag{18}$$

The structure of this iPISMC control is shown in Fig. 4. By substituting equation (18) in equation (11), the closed-loop error is given by:

$$\dot{e} + k_p \cdot e + k_i \cdot \int ed\tau + \alpha \cdot u_e + \tilde{F} = 0 . \tag{19}$$

Define x_1 and x_2 as follows:

$$\begin{cases} x_1 = \int ed\tau \\ x_2 = e \end{cases} , \tag{20}$$

The state-space equations can be obtained as

$$\begin{cases} \dot{x}_1 = x_2 \\ \dot{x}_2 = -k_p * x_2 - k_i * x_1 - \alpha * u_e - \tilde{F} \end{cases} . \tag{21}$$

Therefore, the extra input u_e is designed to compensate the disturbance. According to the sliding mode control framework, a switching function S is defined as

$$S = x_2 + c * x_1 . \tag{22}$$

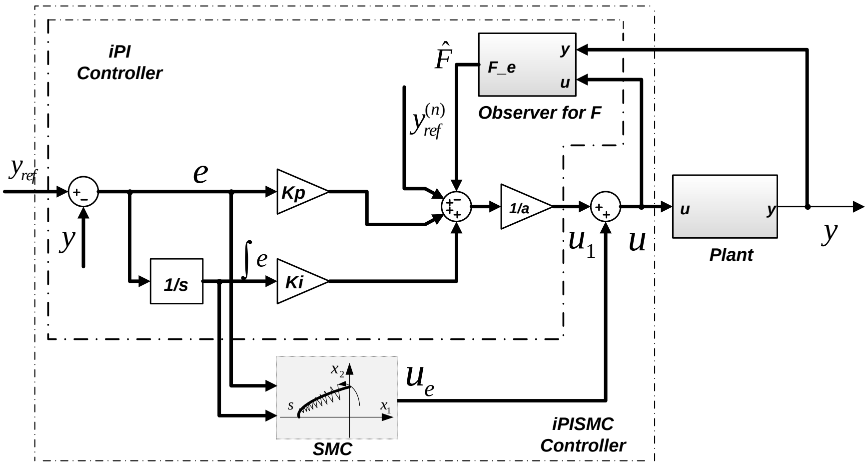

Fig. 4. iPISMC control structure

The derivative of equation (22) is

$$\dot{S} = -k_i * x_1 + (c - k_p)x_2 - \alpha * u_e - \tilde{F} \,. \tag{23}$$

In order to ensure the stability of closed-loop system, the input should be selected so that state trajectories are confined to the sliding hyper surface. The extra input u_e is composed by two parts:

- equivalent control signal u_1 which ensures the ideal sliding mode condition ($S=0$),
- correction control signal u_2 which reduces the chattering effects.

The extra input is

$$u_e = u_1 + u_2 \,. \tag{24}$$

Considering that $\tilde{F}$ is unknown in equation (23) and the ideal sliding mode condition, u_1 is calculated by replacing $\tilde{F}$ with f_m as following

$$u_1 = \frac{1}{\alpha}(-k_i * x_1 + (\mathrm{c} - k_p)x_2 - f_m) \,. \tag{25}$$

In order to reduce the chattering effects, u_2 is selected as

$$u_2 = \frac{1}{\alpha}(\eta_1 * sat(S,\varepsilon) + \eta_2 * S) \,, \tag{26}$$

where $sat(S,\varepsilon) = \begin{cases} 1 & ,S > \varepsilon \\ S/\varepsilon & ,\|S\| \le \varepsilon \\ -1 & ,S < -\varepsilon \end{cases}$ and $\eta_1 > 0$, $\eta_2 > 0$, $\varepsilon > 0$.

The input i_{rq} can be rewritten as follows

$$\begin{aligned} i_{rq}(t) &= \frac{1}{\alpha}(-\hat{F} + \dot{P}^*_{opt} + k_p \cdot e + k_i \cdot \int ed_\tau) + u_e \\ &= \frac{1}{\alpha}(-\hat{F} + \dot{P}^*_{opt} + \eta_1 \cdot sat(S,\varepsilon) + \eta_2 \cdot S + c \cdot e) \end{aligned} \,. \tag{27}$$

3.3 Stability analysis

Define the following Lyapunov function as

$$V = \frac{1}{2}S^2 \,. \tag{28}$$

The derivative of equation (28) is

$$\begin{aligned} \dot{V} &= S\dot{S} = S(\dot{x}_2 + c * \dot{x}_1) \\ &= -S(\eta_1 \cdot sat(S,\varepsilon) + \tilde{F} - f_m) - \eta_2 S^2 \end{aligned} \,. \tag{29}$$

If $S < -\varepsilon$, the boundedness of $\tilde{F}$ is sufficient to ensure that $\dot{V} = -S(-\eta_1 + \tilde{F} - f_m) - \eta_2 S^2 < 0$. If $S > \varepsilon$, $\dot{V} = -S(\eta_1 + \tilde{F} - f_m) - \eta_2 S^2$. According to the boundedness of $\tilde{F}$, it is ensured that $\dot{V} < 0$ if one has $\eta_1 > 2 f_m$.

If $|S| < \varepsilon$, we obtain

$$\dot{V} = -S(\eta_1 S/\varepsilon + \tilde{F} - f_m) - \eta_2 S^2 \,. \tag{30}$$

In order to ensure the negative right-side term, the condition is

$$\begin{aligned} -S(\tilde{F}-f_m)-(\eta_2+\eta_1/\varepsilon)S^2<0 \\ |(\tilde{F}-f_m)|<(\eta_2+\eta_1/\varepsilon)|S| \end{aligned} . \tag{31}$$

Again, given the boundedness of $\tilde{F}$ and $|S|<\varepsilon$, the condition is $(\eta_1+\varepsilon\eta_2)>2f_m$.

In summary, the conditions needed to ensure stability of closed loop system are $\eta_1>2f_m$ and $\eta_2>0, \varepsilon>0$.

The reactive power is related to the d axis rotor current. Usually, the reference of reactive power is set to zero. The structure of reactive power controller can be chosen the same as the above iPISMC control for the active power. Its stability can be proved likewise.

4. Simulation Results

To validate the effectiveness of this proposed iPISMC control, we tested it on the co-simulation platform of Matlab/Simulink and FAST. The main parameters for computer simulations are shown in table 1. The wind turbine model originates in FAST platform which is developed by the National Renewable Energy Laboratory (NREL) [26]. The detailed model and parameters of 5MW DFIG are selected from reference [27].

In this paper, we only investigate three controllers: PI, iPI and iPISMC. The parameters $k_p=5\times10^{-5}$ and $k_i=2.5\times10^{-4}$ are set to the same values for all three methods. This is justified by the fact that iPI is a wrapper for PI and iPISMC is a wrapper for iPI. Moreover, these parameters are optimized using the pole placement method.

4.1 Stochastic wind

In order to demonstrate the performance in more realistic conditions, a stochastic wind has been utilized and the results are shown in Fig. 5. The stochastic wind speed

Table 1. The main parameters of wind turbine system

Parameter Description	Value
Rated Power	*5 MW*
Rotor Radius	*63 m*
Gear Box Ratio	*97*
Moment of inertia	$4.38E+07 N.m^2$
Frequency	*50Hz*
Number of Pole pairs	*3*
Stator resistance	$1.552m\Omega$
Stator Leakage inductance	*1.2721mH*
Rotor resistance	$1.446m\Omega$
Rotor Leakage inductance	*1.1194mH*
Mutual inductance	*5.5182mH*

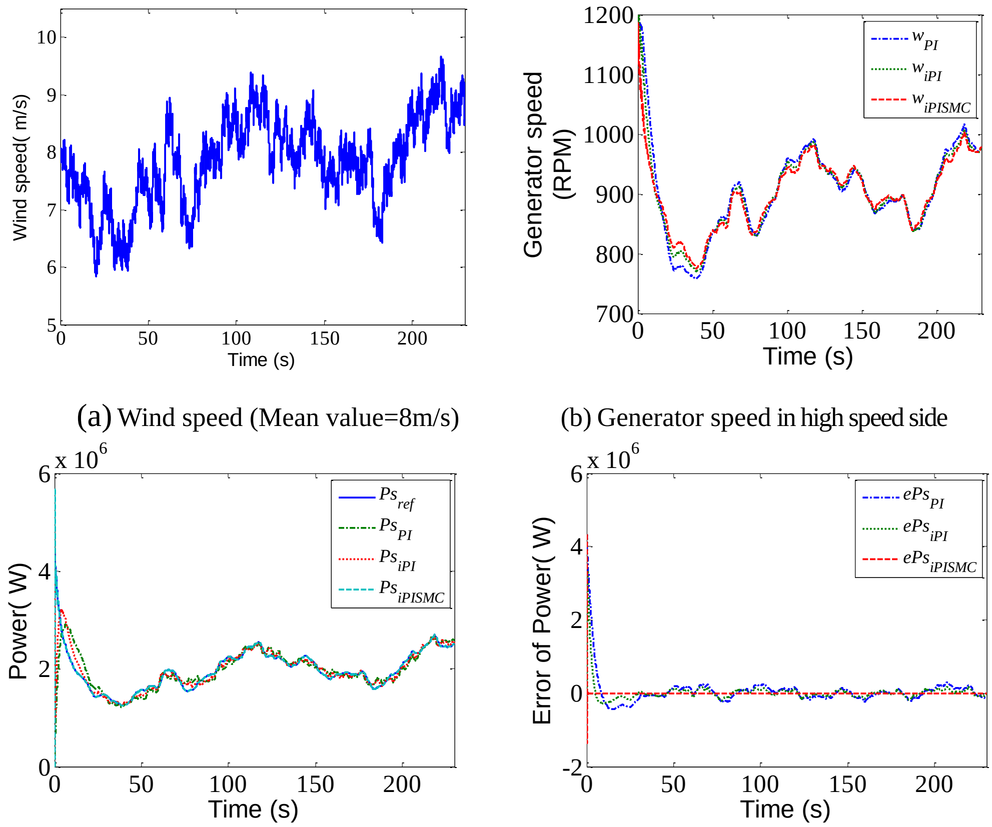

(a) Wind speed (Mean value=8m/s) (b) Generator speed in high speed side

(c) Output power of generator (d) Output power error of generator

Fig. 5. Simulated results with a stochastic wind (mean speed =8 m/s)

mean value is 8.0 m/s. The chosen turbulence model is an international electrotechnical commission (IEC) standard Kaimal model produced by TurbSim software. A realization of that stochastic process is given in Fig. 5(a). Its corresponding tracking performance results are illustrated in Fig. 5 (c-d). It can be noticed clearly from Fig. 5(d) that the proposed iPISMC ensures the best optimal power tracking performance compared with the classical PI and iPI methods.

Table 3. The mean power under PI, iPI and iPISMC

(Mean value=8m/s, IEC standard Kaimal model)

Criterions	*k_p=5.0×10^{-5} k_i=2.5×10^{-4}*			*k_p=1.9×10^{-5} k_i=9.3×10^{-4}*			*k_p=1.0×10^{-4} k_i=5.1×10^{-4}*		
	PI	*iPI*	*iPISMC*	*PI*	*iPI*	*iPISMC*	*PI*	*iPI*	*iPISMC*
Mean power (value ×10^5)	*1.9759*	*1.9801*	*1.9834*	*1.9586*	*1.9727*	*1.9834*	*1.9802*	*1.982*	*1.9834*
Mean error of power error (value ×10^5)	*0.4705*	*0.2268*	*0.0007*	*1.3228*	*0.6453*	*0.0007*	*0.2218*	*0.1089*	*0.0007*
Variance of power error (value ×10^{11})	*1.6456*	*0.7441*	*0.0102*	*4.6253*	*2.1684*	*0.0102*	*0.7856*	*0.3451*	*0.0102*

A complementary numerical analysis is provided by table 3. Different controller parameters are selected and tested. Comparing PI with iPI under the same conditions, the mean power using iPI is bigger than that of PI, while the mean error and variance

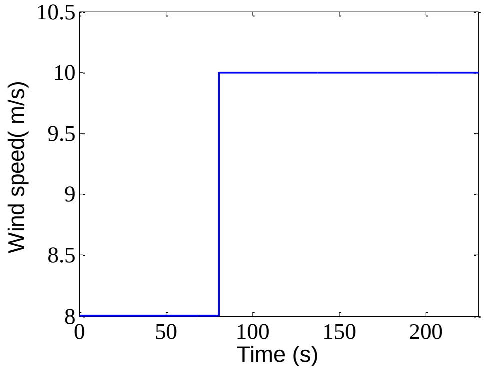

(a) Wind speed

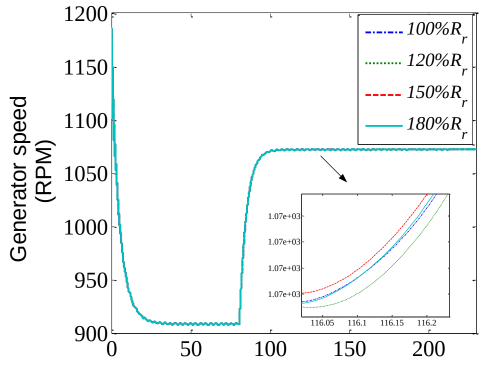

(b) Generator speed in the high speed side

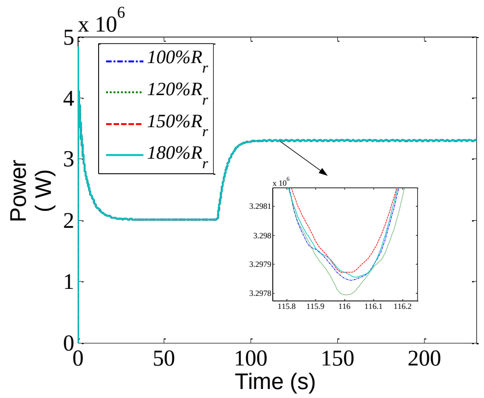

(c) Output power of generator

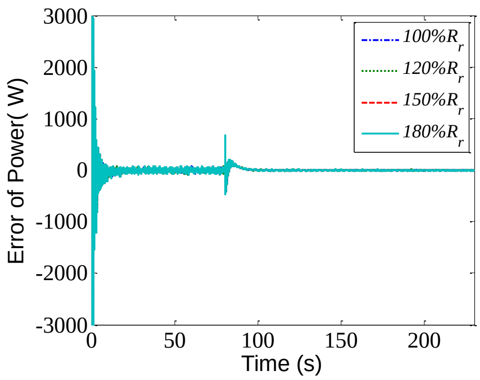

(d) Output power error of generator

Fig. 6. Simulation results with R_r =100% 120% 150% and 180%

are smaller. With the same parameters k_p and k_i, the mean power obtained when using iPISMC is bigger than that of other methods. Furthermore, the values of mean error and variance reflect iPISMC efficiency. It shows that iPISMC also outperforms PI and iPI controllers regarding this criterion.

4.2 Step wind with parameter variations

In order to test the influence of DFIG parameter variations on the performances of the proposed iPISMC, different conditions with parameter variation of resistances and mutual inductance have been tested and the corresponding results are reported in Fig. 6 - 8. For instance, the resistance is sensitive to the temperature which changes gradually with respect to ambient temperature. Consequently, the rotor resistances and mutual inductance are considered and tested.

Fig. 6-8 respectively shows the results of generator rotor speed, power and its tracking error under the variations of resistances $a \cdot R_r$, $a \cdot R_s$ and the mutual inductance with $a \cdot L_m$ with $a = \{1;1.2;1.5;1.8\}$.

From the figures, the power errors converge to zero rapidly. Parameter variations have no significant influence on output rotor speed or power. From these results, one can notice that our iPISMC is robust and able to reject the influences of the variations of system parameters.

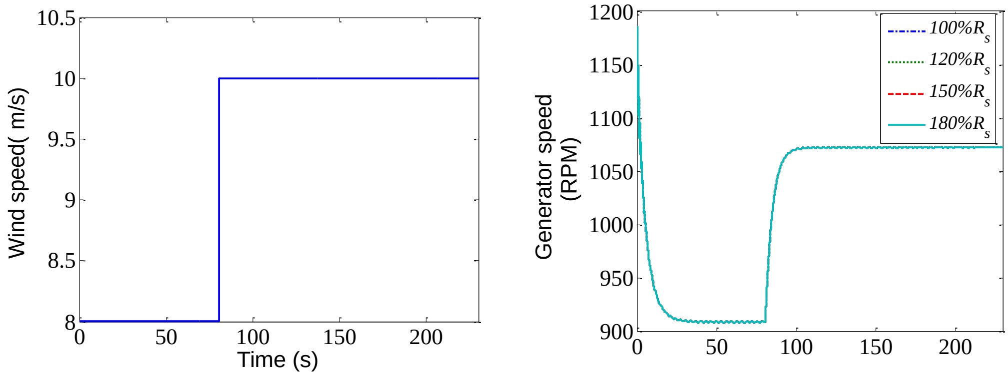

(a) Wind speed (b) Generator speed in the high speed side

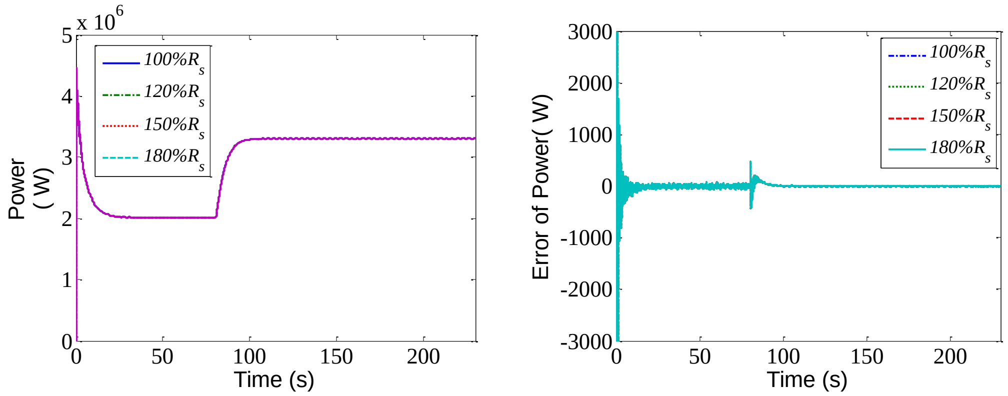

(c) Output power of generator (d) Output power error of generator

Fig. 7. Simulation results with R_S = 100% 120% 150% and 180%

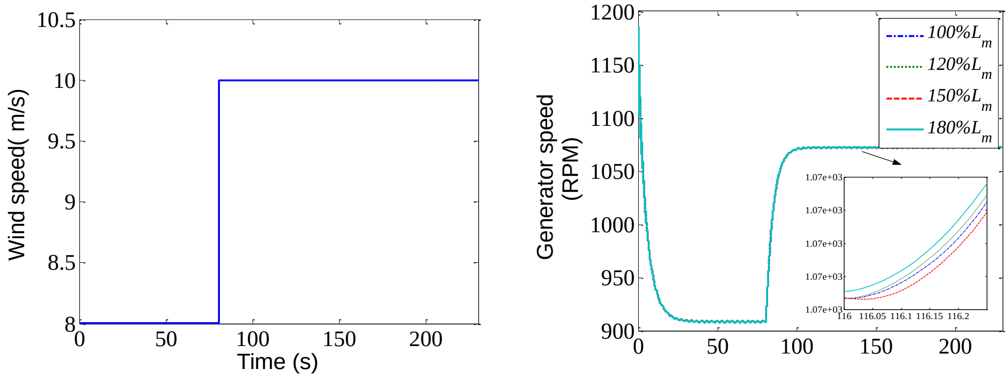

(a) Wind speed (b) Generator speed in the high speed side

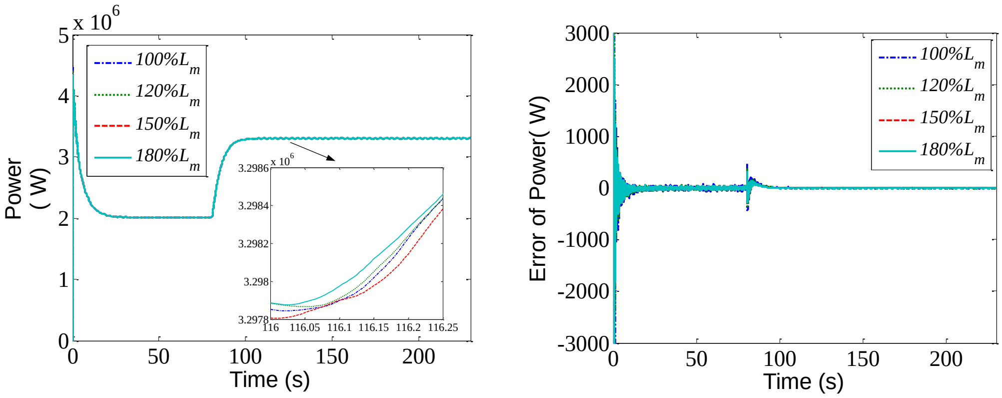

(c) Output power of generator (d) Output power error of generator

Fig. 8. Simulation results with Lm = 100% 120% 150% and 180%

5. Conclusion

In this paper, an intelligent proportional-integral sliding mode control for direct power control of variable speed-constant frequency wind turbine system is presented. This controller consists in two nested controllers: an intelligent proportional integral controller enhanced by a sliding mode compensated controller. In order to demonstrate its performance, the controller is tested in two different cases which include stochastic wind and parameter variations.

Under stochastic wind turbulences, the average output error of iPISMC is significantly smaller than that of PI or iPI. Moreover, iPISMC is not sensitive to unpredictable parameter variations. This also tends to show that iPISMC can be employed when these parameters are ill-known. Consequently, iPISMC is well suited for DFIG wind turbine robust control in practical situations.

Acknowledgments

This work is supported by National Nature Science Foundation of China(61304077, 61203115), Jiangsu Province under Grant(BK2013075), by the Chinese Ministry of Education Project of Humanities and Social Sciences (13YJCZH171), by the Funding of Jiangsu Innovation Program for Graduate Education(Grant No.KYLX 0377)

References

[1] Mani S, Dhingra T. Critique of offshore wind energy policies of the UK and Germany—What are the lessons for India. Energy Policy. 2013, 63, 900-9.

[2] Lo K. A critical review of China's rapidly developing renewable energy and energy efficiency policies. Renewable & Sustainable Energy Reviews. 2014, 29, 508-16.

[3] Fadaeinedjad R, Moallem M, Moschopoulos G. Simulation of a wind turbine with doubly-fed induction generator by FAST and Simulink. IEEE Transactions on Energy Conversion. 2008, 23, 1-.

[4] Cárdenas R, Peña R, Alepuz S, Asher G. Overview of control systems for the operation of DFIGs in wind energy applications. IEEE Transactions on Industrial Electronics. 2013, 7,

2776-98.

[5] Bourdoulis MK, Alexandridis AT. Direct Power Control of DFIG Wind Systems Based on Nonlinear Modeling and Analysis. IEEE Journal of Emerging & Selected Topics in Power Electronics. 2014, 2, 764-75.

[6] Hu J, Nian H, Hu B, He Y. Direct Active and Reactive Power Regulation of DFIG Using Sliding-Mode Control Approach. IEEE Transactions on Energy Conversion. 2010, 25, 1028-39.

[7] Kamal E, Oueidat M, Aitouche A, Ghorbani R. Robust Scheduler Fuzzy Controller of DFIG Wind Energy System. IEEE Transactions on Sustainable Energy. 2013, 4, 706-15.

[8] Pichan M, Rastegar H, Monfared M. Two fuzzy-based direct power control strategies for doubly-fed induction generators in wind energy conversion systems. Energy. 2013, 51, 154-62.

[9] Jafarnejadsani H, Pieper J, Ehlers J. Adaptive Control of a Variable-Speed Variable-Pitch Wind Turbine Using Radial-Basis Function Neural Network. IEEE Transactions on Control Systems Technology. 2013, 21, 2264-72.

[10] Poultangari I, Shahnazi R, Sheikhan M. RBF neural network based PI pitch controller for a class of 5-MW wind turbines using particle swarm optimization algorithm. ISA Transactions. 2012, 51, 641-8.

[11] Beltran B, Ahmed-Ali T, Benbouzid M. High-Order Sliding-Mode Control of Variable-Speed Wind Turbines. IEEE Transactions on Industrial Electronics. 2009, 56, 3314-21.

[12] Torchani B, Sellami A, Garcia G. Variable speed wind turbine control by discrete-time sliding mode approach. ISA Transactions.

[13] Fliess M, Join C. Intelligent PID controllers. 16th Mediterrean Conference on Control and Automation2008.

[14] Al Younes Y, Drak A, Noura H, Rabhi A. Model-free control of a quadrotor vehicle. The 2014 International Conference on Unmanned Aircraft Systems, ICUAS'142014. p. 1126-31.

[15] Michel L, Join C, Fliess M, Sicard P, Chériti A. Model-free control of dc/dc converters. 2010 IEEE 12th Workshop on Control and Modeling for Power Electronics (COMPEL), 2010. p. 1-8.

[16] Fliess M, Join C. Model-free control. International Journal of Control. 2013, 86, 2228-52.

[17] Fliess M, Join C, Sira-Ramirez H. Complex continuous nonlinear systems: their black box identification and their control. Proc 14th IFAC Symposium on System Identification (SYSID 2006)2006.

[18] Freidovich LB, Khalil HK. Performance recovery of feedback-linearization-based designs. IEEE Transactions on Automatic Control. 2008, 53, 2324-34.

[19] Lin W-M, Hong C-M. Intelligent approach to maximum power point tracking control strategy for variable-speed wind turbine generation system. Energy. 2010, 35, 2440-7.

[20] Abdeddaim S, Betka A. Optimal tracking and robust power control of the DFIG wind turbine. International Journal of Electrical Power & Energy Systems. 2013, 49, 234-42.

[21] Wang Z, Sun Y, Li G, Li X. A Novel Control Strategy for DFIG Based on Magnitude and Frequency of Rotor Voltage for Wind Power Generation. Asia-Pacific Power and Energy Engineering Conference, 2009 APPEEC 20092009. p. 1-7.

[22] Inthamoussou FA, Bianchi FD, De Battista H, Mantz RJ. LPV Wind Turbine Control With Anti-Windup Features Covering the Complete Wind Speed Range. IEEE Transactions on Energy Conversion. 2014, 29, 259-66.

[23] Kairous D, Wamkeue R. DFIG-based fuzzy sliding-mode control of WECS with a flywheel energy storage. Electric Power Systems Research. 2012, 93, 16-23.

[24] Petersson A, Harnefors L, Thiringer T. Comparison between stator-flux and grid-flux-oriented rotor current control of doubly-fed induction generators. 2004 IEEE 35th Annual Power Electronics Specialists Conference, 2004 PESC 04 IEEE2004. p. 482-6.

[25] Guo B-Z, Zhao Z-l. On the convergence of an extended state observer for nonlinear systems with uncertainty. Systems & Control Letters. 2011, 60, 420-30.

[26] Jonkman JM, Butterfield S, Musial W, Scott G. Definition of a 5-MW reference wind turbine for offshore system development. National Renewable Energy Laboratory Golden, CO, USA2009.

[27] Wu B, Lang Y, Zargari N, Kouro S. Power conversion and control of wind energy systems. John Wiley & Sons2011.